High cancer susceptibility and embryonic lethality associated with mutation of the *PTEN* tumor suppressor gene in mice

Akira Suzuki, José Luis de la Pompa, Vuk Stambolic, Andrew J. Elia, Takehiko Sasaki, Iván del Barco Barrantes, Alexandra Ho, Andrew Wakeham, Annick Itie, Wilson Khoo, Manabu Fukumoto* and Tak W. Mak

Background: Germ-line and sporadic mutations in the tumor suppressor gene *PTEN* (also known as *MMAC* or *TEP1*), which encodes a dual-specificity phosphatase, cause a variety of cancers such as Cowden disease, glioblastoma, endometrial carcinoma and prostatic cancer. *PTEN* is widely expressed, and Cowden disease consistently affects various organ systems, suggesting that the PTEN protein must have an important, although as yet poorly understood, function in cellular physiology.

Results: Homozygous mutant mice lacking exons 3–5 of the *PTEN* gene (*mPTEN*$^{3-5}$) had severely expanded and abnormally patterned cephalic and caudal regions at day 8.5 of gestation. Embryonic death occurred by day 9.5 and was associated with defective chorio-allantoic development. Heterozygous *mPTEN*$^{3-5}$ mice had an increased incidence of tumors, especially T-cell lymphomas; γ-irradiation reduced the time lapse of tumor formation. DNA analysis of these tumors revealed the deletion of the *mPTEN* gene due to loss of heterozygosity of the wild-type allele. Tumors associated with loss of heterozygosity in *mPTEN* showed elevated phosphorylation of protein kinase B (PKB, also known as Akt kinase), thus providing a functional connection between *mPTEN* and a murine proto-oncogene (*c-Akt*) involved in the development of lymphomas.

Conclusions: The *mPTEN* gene is fundamental for embryonic development in mice, as *mPTEN*$^{3-5}$ mutant embryos died by day 9.5 of gestation, with patterning defects in cephalic and caudal regions and defective placentation. Heterozygous mice developed lymphomas associated with loss of heterozygosity of the wild-type *mPTEN* allele, and tumor appearance was accelerated by γ-irradiation. These lymphomas had high levels of activated Akt/PKB, the protein product of a murine proto-oncogene with anti-apoptotic function, associated with thymic lymphomas. This suggests that tumors associated with *mPTEN* loss of heterozygosity may arise as a consequence of an acquired survival advantage. We provide direct evidence of the role of *mPTEN* as a tumor suppressor gene in mice, and establish the *mPTEN* mutant mouse as an experimental model for investigating the role of *PTEN* in cancer progression.

Addresses: Amgen Institute, Ontario Cancer Institute and Department of Medical Biophysics and Immunology, University of Toronto, Toronto, Ontario, Canada M5G 2C1. *Department of Pathology, Institute of Development, Aging and Cancer, Tohoku University, Sendai, Japan 980-8575.

Correspondence: Tak W. Mak
E-mail: t.mak@oci.utoronto.ca

Received: 7 August 1998
Revised: 21 September 1998
Accepted: 22 September 1998

Published: 5 October 1998

Current Biology 1998, 8:1169–1178
http://biomednet.com/elecref/0960982200801169

Background

PTEN was recently cloned as a tumor suppressor gene at chromosomal location 10q23.3 [1–3]. Somatic mutations or homozygous deletion of *PTEN* have been found in various kinds of primary malignant tumors [4], such as glioblastoma (20–75%) [4–6], prostatic cancer (10–49%) [7,8], small-cell lung cancer (40%) [9], endometrial cancer (34–50%) [10,11], breast cancer [12,13], and anaplastic meningiomas [14]. A significantly higher rate of loss of heterozygosity or mutations was observed in the more advanced stage of malignant tumors (glioma, prostatic cancer and breast cancer) [8,13,15] or in tumor cell lines [4], suggesting that *PTEN* may be involved in tumor progression rather than in initiation. Germ-line mutations in the *PTEN* gene cause Cowden disease [16,17], a rare autosomal dominant syndrome, characterized by multiple hamartomas of the skin, intestine, breast and thyroid and increased risk of breast, thyroid and brain tumors [18].

PTEN encodes a dual-specificity protein phosphatase [19], and also shows homology to tensin and auxillin, cytoskeletal proteins that interact with adhesion molecules. The PTEN protein has been reported to dephosphorylate position D3 of phosphatidylinositol

Figure 1

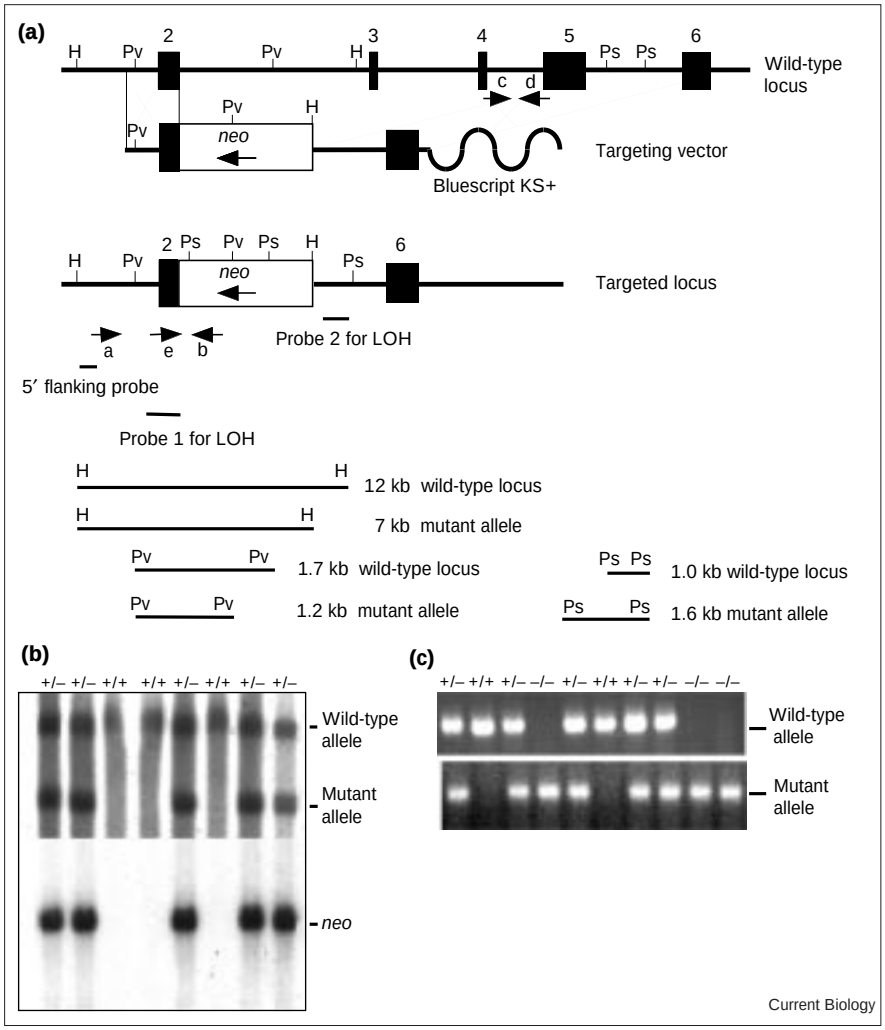

Targeted disruption of the *mPTEN* locus. (a) The top line shows a portion of the *mPTEN* locus comprising exons 2 to 6 and the locations of the PCR primers c and d used to identify the wild-type allele. The targeting vector with the neomycin-resistance gene (*neo*) in antisense orientation to *mPTEN* gene transcription is shown below. The targeting vector was designed such that the *neo* cassette replaced exons 3, 4 and 5 and the splice donor site of exon 2 of *mPTEN*. Diagrammed below is the targeted *mPTEN* locus showing how the mutant 7 kb *Hind*III fragment is created. The locations of other restriction fragments that are diagnostic of wild-type or mutant alleles are also shown. The position of the 5′ flanking probe used for genotyping by Southern analysis is shown, as are the locations of probes 1 and 2 for loss-of-heterozygosity (LOH) studies and the PCR primers a and b, or e and b, which were used to identify the mutant allele. (b) Southern blot analysis of genomic tail DNA from one representative litter of *mPTEN*$^{3–5}$ heterozygous intercrosses. DNA was digested with *Hind*III and hybridized with the 5′ flanking probe (upper panel) and the *neo* probe (lower panel). Using the 5′ flanking probe, a 12 kb band representative of the wild-type allele and a 7 kb band of the mutated allele were detected. A single 7 kb band was obtained using the *neo* probe and no random integrations were detected. (c) Representative genotyping of an embryonic litter from *mPTEN*$^{3–5}$ heterozygous intercross. DNA samples were subjected to PCR using the primer pairs e/b and c/d. PCR amplification of the wild-type *mPTEN* allele by primer pair c/d yields a 669 bp fragment (upper panel), whereas PCR amplification of the mutated *mPTEN* allele by pair e/b yields a 144 bp fragment (lower panel). H, *Hind*III; Pv, *Pvu*II; Ps, *Pst*I.

3,4,5-trisphosphate (PtdIns(3,4,5)P_3) [20], a direct product of phosphatidyl-inositol 3′-kinase (PI3K) activity, and PtdIns(3,4,5)P_3 has been previously shown to regulate PDK1, a kinase that phosphorylates Akt/PKB [21], the protein product of a proto-oncogene involved in anti-apoptotic [16,22] mechanisms. Overexpression of wild-type PTEN suppresses growth in *PTEN*-mutated glioblastoma [23]; moreover, overexpressed PTEN interacts directly with focal adhesion kinase (FAK), reducing its tyrosine phosphorylation, and eventually inhibiting cell migration, integrin-mediated cell spreading and formation of focal adhesions [24]. Thus, PTEN may control the interaction between extracellular matrix and cytoskeleton, and be involved in infiltration or metastasis of malignant cells. The importance of an intact PTEN phosphatase domain for its tumor suppressor function is underscored by the finding that a large proportion of tumor-associated *PTEN* mutations map to the region encoding the phosphatase domain [6,25]. Furthermore, phosphatase-dead mutants are unable to reduce the tyrosine phosphorylation of FAK or reduce the PtdIns(3,4,5)P_3 level and, unlike wild-type PTEN, catalytically inactive PTEN is unable to suppress growth and tumorigenicity of PTEN-deficient glioblastoma cells [23].

To determine the role of PTEN in normal development and tumorigenesis, we have generated mice with a targeted deletion of exons 3 to 5 of the *PTEN* gene (*mPTEN*$^{3–5}$). Homozygous *mPTEN*$^{3–5}$ mutant mice died by embryonic day 9.5 (E9.5) and showed abnormally patterned and expanded cephalic and caudal regions. Heterozygous *mPTEN*$^{3–5}$ mice had a high incidence of lymphomas associated with loss of heterozygosity of the wild-type *PTEN* allele; appearance of tumors was

accelerated by γ-irradiation. These tumors showed elevated phosphorylation of Akt/PKB, providing a functional connection between the murine *PTEN* gene and an oncogene involved in the development of lymphomas.

Results

Generation of *mPTEN*$^{3-5}$ mutant mice

We disrupted the murine *PTEN* (*mPTEN*) locus by homologous recombination in embryonic stem (ES) cells, using a targeting vector that deleted the splice donor site of exon 2 and the whole of exons 3 to 5, thus deleting the phosphatase domain encoded in exon 5. A neomycin-resistance gene (*neo*) with the phosphoglycerokinase (*PGK*) promoter and a poly(A) addition signal was inserted in the targeting vector in antisense orientation to *mPTEN* transcription, so that the short arm of the vector consisted of a 732 bp PCR-amplified fragment of *mPTEN* that included the splice donor site of exon 2 and the long arm contained 11.9 kb of an *ApaI* fragment that included exon 6. Insertion of *neo* generates stop codons in all reading frames; therefore, protein sequences beyond the beginning of exon 6 are not expected to be translated (Figure 1a). PCR and Southern blot analysis of ES cells electroporated with the targeting construct showed that 6 out of 3200 G418-resistant colonies were heterozygous for the *mPTEN* locus with no random integration. Three out of six ES cell clones used to generate chimeric mice gave germ-line transmission.

Developmental delay of E7.5 *mPTEN*$^{3-5}$ mutant embryos

No viable homozygous mutant pups were born among 50 offspring from heterozygous intercrosses, indicating that homozygosity for the *mPTEN*$^{3-5}$ mutation causes embryonic lethality (Figure 1b). To determine the consequences of the *mPTEN*$^{3-5}$ mutation on embryonic development, we analyzed embryos from heterozygous intercrosses at different days of gestation. At E7.5, wild-type embryos have a well-organized anteroposterior (AP) pattern and are about to begin organogenesis (Figure 2a). In contrast, E7.5 *mPTEN*$^{3-5}$ mutant embryos (6 embryos out of 28) appeared less advanced, and their germ layers were not distinct, which is characteristic of early embryonic stages (Figure 2b). Histological analysis revealed that, whereas normal embryos show well-defined germ layers and primordia of the headfold and allantois (Figure 2c), *mPTEN*$^{3-5}$ homozygous mutant embryos developed ectoderm and a morphologically distinct mesoderm, but appeared more compact and less organized (Figure 2d). The generation of mesoderm was confirmed by *in situ* hybridization analysis of the expression of the early gastrulation marker *Brachyury* [26] (data not shown). Immunostaining with an anti-mPTEN antiserum [27] revealed ubiquitous mPTEN expression at E7.5 (data not shown), consistent with our northern blot analysis (see below). Homozygous mutant *mPTEN*$^{3-5}$ embryos showed no staining (data not shown), indicating that the *mPTEN*$^{3-5}$ mutation is very likely to be a loss-of-function mutation.

Figure 2

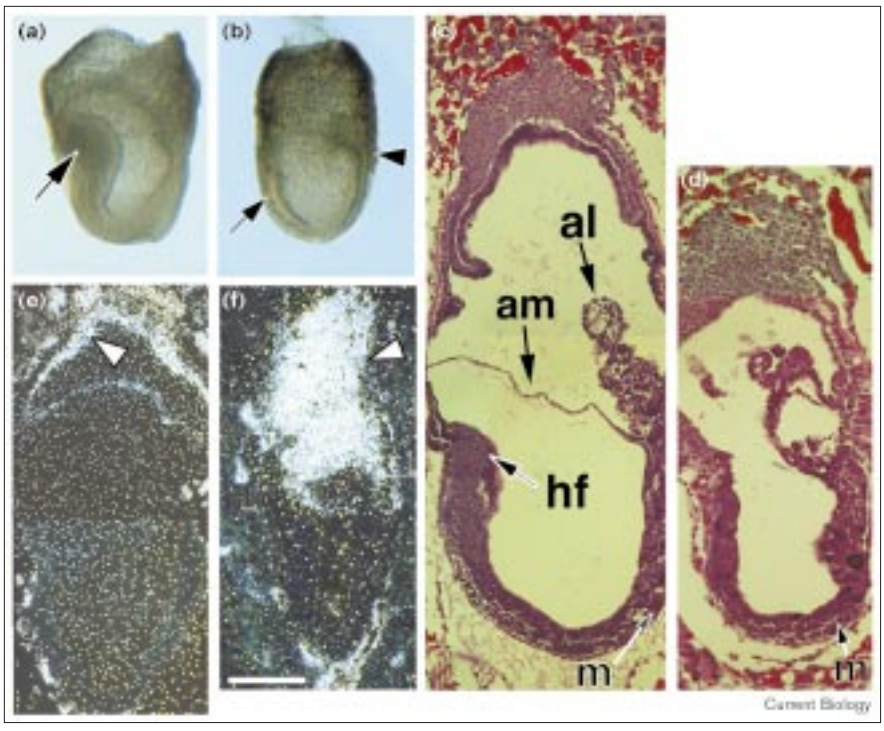

E7.5 *mPTEN*$^{3-5}$ mutant embryos appear developmentally delayed. **(a)** Wild-type embryo, whole mount. Note the developing headfolds in the anterior region of the embryo (arrow). **(b)** *mPTEN*$^{3-5}$ homozygous mutant embryo. The arrow points to the poorly organized anterior region of the embryo and the arrowhead demarcates the junction between the embryonic and extraembryonic regions. **(c,d)** Hematoxylin and eosin staining of (c) a wild-type and (d) a *mPTEN*$^{3-5}$ mutant embryo. In the wild type (c), the headfolds (hf) are developing, the mesoderm (m) is expanding, the allantois (al) grows in the caudal region, and the amnion (am) is apparent. In the mutant (d), organization is more primitive and cephalic and caudal structures are undefined, although the developing mesoderm (m) is clearly visible. **(e,f)** Radioactive *in situ* hybridization; dark-field images showing (e) *Mash2* expression in the ectoplacental cone (arrowhead) of a wild-type embryo and (f) expansion of *Mash2* expression into the entire extraembryonic region (arrowhead) in a *mPTEN*$^{3-5}$ mutant embryo, a pattern normally observed at E6.5. Panels c–f are sagittal sections. Anterior is to the left. Bar represents 140 μm in (a,b) and 70 μm in (c–f).

The development of the extraembryonic lineages in *mPTEN*$^{3-5}$ mutants was examined by looking at the expression of *Mash2*, a diploid trophoblast marker [28,29]. At E7.5, *Mash2* is normally only detected in the ectoplacental cone (Figure 2e), but *mPTEN*$^{3-5}$ mutant embryos expressed *Mash2* in the trophoblast lineage (Figure 2f), a pattern normally observed at E6.5. Taken together, these data indicate that early gastrulation and extraembryonic lineage specification appear to occur normally in *mPTEN*$^{3-5}$ mutant embryos.

Abnormal patterning in E8.5 *mPTEN*$^{3-5}$ mutant embryos

At E8.5, 22 out of a total of 39 (56%) *mPTEN*$^{3-5}$ mutant embryos analyzed were still alive and showed severe defects in anterior and posterior development. E8.5 wild-type embryos have by this stage undergone chorio-allantoic fusion and have established the connection between the maternal and embryonic circulation (Figure 3a). In contrast, *mPTEN*$^{3-5}$ mutant embryos failed to connect allantois and chorion, and instead displayed an expanded, loose and disorganized allantois (Figure 3b). In addition, the cephalic region also showed extremely prominent and disproportionate headfolds (Figure 3b–d). Although AP axis elongation appeared fairly normal, somites in *mPTEN*$^{3-5}$ mutant embryos were fewer and less distinct than in wild-type littermates (Figure 3b–d). At E9.5, *mPTEN*$^{3-5}$ mutant embryos were dead and started to be resorbed.

To determine if these abnormalities are the consequence of a patterning defect, we analyzed the expression of markers specific for these embryonic regions. Figure 3e shows the normal striped expression of the hindbrain marker *Krox20* at E8.5 [30], and the metameric distribution of the paraxial mesoderm marker *Mox1* [31]. Mutant *mPTEN*$^{3-5}$ embryos showed abnormal *Krox20* expression on one side of the prospective forebrain region (Figure 3f). *Mox1* was expressed in *mPTEN*$^{3-5}$ mutant embryos (Figure 3f), although somites appeared more compact and less defined. *Wnt1* expression is normally restricted to the midbrain and the dorsal region of the developing neural tube [32] (Figure 3g). In *mPTEN*$^{3-5}$ mutant embryos, *Wnt1* expression was observed in the severely deformed head folds in the cephalic region, but not in the neural tube (Figure 3h). The primitive-streak marker *Wnt3a* is normally expressed in the tail bud region [33] (Figure 3i). Mutant *mPTEN*$^{3-5}$ embryos showed reduced *Wnt3a* expression (Figure 3j), suggesting a defect in the generation of mesodermal lineages. These results indicate that patterning in the cephalic and caudal regions of *mPTEN*$^{3-5}$ mutant embryos is disturbed.

Untreated or irradiated heterozygous *mPTEN*$^{3-5}$ mice are susceptible to tumors

Germ-line mutations at the *PTEN* locus are found in Cowden disease, and affected individuals are susceptible to hamartomas of the skin, intestine, breast and thyroid, and are at high risk for breast cancer, thyroid cancer and brain tumors [16]. In the mouse, northern blot analysis revealed that in addition to being expressed throughout

Figure 3

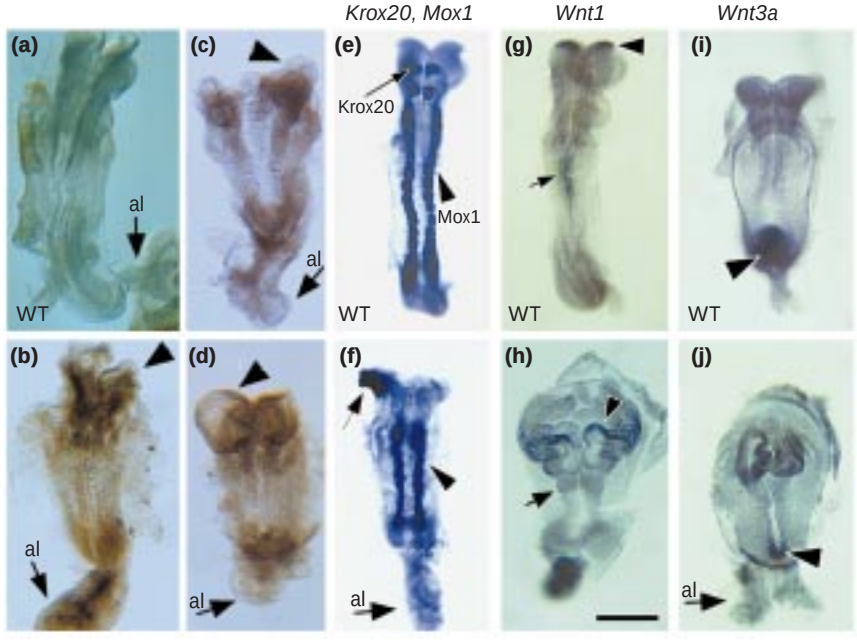

Abnormal patterning in E8.5 *mPTEN*$^{3-5}$ mutant embryos. **(a)** Wild-type (WT) embryo. AP pattern is well organized, and the allantois (al) is fused to the chorion. **(b–d)** Mutant *mPTEN*$^{3-5}$ embryos. Severe overgrowths of the cephalic region (arrowhead) and allantois (arrow) were observed. The latter never fused with the chorion. **(e,f)** *In situ* hybridization to detect *Krox20* (arrow) and *Mox1* (arrowhead) expression in (e) wild-type and (f) *mPTEN*$^{3-5}$ mutant embryos. In (f), abnormal *Krox20* expression was found in only one deformed headfold; *Mox1* expression in the compact paraxial mesoderm identified the poorly defined somites. **(g,h)** *Wnt1* expression in (g) the wild-type embryo is detectable in the midbrain (arrowhead) and in the dorsal region of the neural tube (arrow); in (h) the *mPTEN*$^{3-5}$ mutant embryo, *Wnt1* is expressed in the presumptive midbrain region (arrowhead) but not in the dorsal neural tube. The arrow in (h) points to an ectopic headfold. **(i,j)** *Wnt3a* is strongly expressed in the tail bud region (arrowhead) in (i) the wild-type embryo but is reduced in the corresponding region in (j) the *mPTEN*$^{3-5}$ embryo. Note hypertrophic allantois in (b–d,f,j). Bar = 200 μm and applies to all panels.

embryogenesis (Figure 4a), two major *mPTEN* transcripts of approximately 2.5 kb and 5 kb in size are expressed in a variety of adult tissues (Figure 4b), indicating that *mPTEN* has a role in differentiated organs.

To determine whether *mPTEN* is a tumor suppressor gene in the mouse, we monitored *mPTEN*$^{3-5}$ heterozygous mice for tumor development. In total, spontaneous tumors occurred in 9 out of 66 (14%) heterozygous mutant mice (Table 1). In most cases, mice were sacrificed because of enlargement of the cervical or axillary lymph nodes. Interestingly, 8 out of 9 tumors (88%) showed lymphoma/leukemia of the T-cell type (Figure 5a–c) as assessed by flow cytometric analysis (Table 1). Also observed were three cases (33%) of atypical adenomatous hyperplasia in the liver (Figure 5d), a borderline lesion of hepatocellular carcinoma. In addition, we observed three cases (33%) of teratocarcinoma (Figure 5e,f), and one case (11%) of prostatic cancer (Figure 5g). Microscopic hamartomatous polyps mainly in the colon, and focal atrophic changes in the seminiferous tubules, were observed in most of the mice examined (data not shown). During the period of observation, however, none of the mice developed brain tumors, thyroid cancer or breast cancer such as seen in Cowden disease in humans. Overall, 14% of the heterozygous mice developed tumors during the 28 weeks of observation, whereas no tumors were observed in 50 wild-type mice during the same time. Southern blot analysis using 'probe 1' and 'probe 2' (see Figure 1a) showed either a complete or partial (due to contamination with normal tissue) loss of wild-type *mPTEN* allele in two out of eight untreated mice examined (Figure 5j). Loss of heterozygosity due to point mutations or small deletions was not tested; thus the frequency of loss of heterozygosity may be an underestimate.

Radiation-induced carcinogenesis was also examined using 30 wild-type and 32 heterozygous mice exposed to a single dose of 5 Gy whole-body γ-irradiation at 5–6 weeks of age and monitored for a mean of 20 weeks after birth. Six out of 32 heterozygous mice (19%) developed tumors in the irradiated group, whereas none of the irradiated wild-type mice developed tumors over the same period (Table 1). Unlike the untreated group, tumor-bearing irradiated heterozygous *mPTEN*$^{3-5}$ mice were found dead or were sacrificed because of labored breathing. Autopsy revealed a markedly enlarged thymus displacing the heart and lungs to the posterior of the thoracic region. Histological analysis showed that these tumors were thymic lymphomas/leukemias (Figure 5h,i). Thus, irradiation significantly decreased the latency period for tumor development ($p = 0.017$ by log-rank test); moreover, all of the tumors in the irradiated group showed loss of heterozygosity of the *mPTEN* locus (Table 1), suggesting that *mPTEN* is one of the target genes of radiation tumorigenesis.

Figure 4

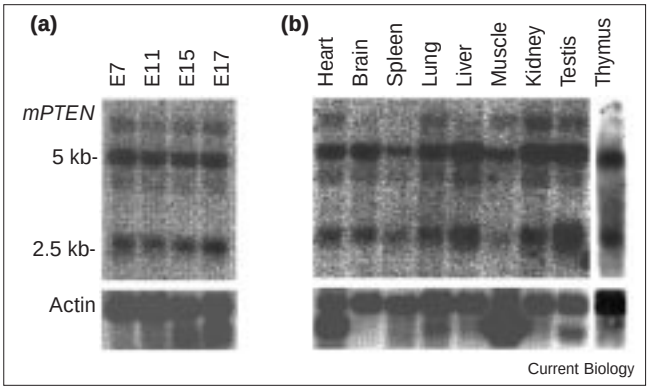

The *mPTEN* gene is expressed throughout embryogenesis and ubiquitously in the adult. Northern blot analysis of poly A$^+$ RNA or 30 μg total RNA (thymus), hybridized with a full-length *mPTEN* cDNA probe or with a probe for *β-actin,* as a control for sample loading. Two *mPTEN* transcripts of 2.5 kb and 5 kb were detected in (a) embryos and (b) adult tissues, particularly in liver and thymus.

Increased phosphorylation of Akt/PKB in tumors with loss of heterozygosity at the *mPTEN* locus

The viral oncogene v-*akt*, which consists of a viral *gag* sequence fused to the entire open reading frame of the murine *Akt/PKB* gene, causes T-cell lymphomas in mice [22]. We have demonstrated that mPTEN is a negative regulator of Akt/PKB-mediated cell survival [27]; we therefore examined the Akt/PKB phosphorylation status in *mPTEN* thymomas associated with loss of heterozygosity. Akt/PKB phosphorylation was greatly elevated in these thymomas in comparison with normal thymus, which exhibited undetectable levels of Akt/PKB phosphorylation (Figure 6). Thymic lymphomas associated with *mPTEN* loss of heterozygosity showed reduced Akt/PKB protein levels, possibly due to degradation or proteolytic cleavage [34]. Thus, these thymomas may arise through the same mechanism as those induced by *AKT8*, a murine retrovirus carrying v-*akt*.

Discussion

Abnormal cephalic and caudal patterning in *mPTEN*$^{3-5}$ mutant embryos

We have generated a null mutation in the *mPTEN* gene by homologous recombination in ES cells. In contrast to a recent report by Cristofano *et al.* [35], in which the *in vitro* differentiation potential of *mPTEN* mutant ES cells was analyzed, we provide an *in vivo* developmental characterization of the *mPTEN* mutant phenotype.

We found that E7.5 *mPTEN*$^{3-5}$ mutant embryos undergo gastrulation, although they appear less advanced and less well organized than their wild-type littermates. At E8.5, surviving *mPTEN*$^{3-5}$ mutants were relatively smaller than their wild-type littermates, and showed defective patterning of the cephalic and caudal regions, as

Table 1

Tumors in *mPTEN*$^{3-5}$ mutant mice.

Mouse	Age (weeks)	Histology	Thymus	Lymph node	Spleen	Bone marrow	Liver	Kidney	Lung	LOH
(a) Untreated group										
1	8	*Teratocarcinoma (peritoneal cavity) Microscopic hamartomatous polyps (colon)								n.d.
2	17	*Lymphoma/leukemia (T-cell) Atypical adenomatous hyperplasia (liver) Microscopic hamartomatous polyps (colon)	+	++	+	–	+	+		–
3	17	*Lymphoma/leukemia (T-cell) Atypical adenomatous hyperplasia (liver) Microscopic hamartomatous polyps (colon)	++	+	+	+	+		+	+
4	22	*Lymphoma/leukemia (T-cell) Microscopic hamartomatous polyps (colon)		++	+	–	–	–	–	–
5	25	*Lymphoma/leukemia (T-cell) Microscopic hamartomatous polyps (colon)		++	+	–			+	–
6	28	*Lymphoma/leukemia (T-cell)		++			–	+	+	–
7	30	*Lymphoma/leukemia (T-cell) Teratocarcinoma (uterus) Atypical adenomatous hyperplasia (liver) Microscopic hamartomatous polyps (colon)		++	+	–			+	–
8	31	*Lymphoma/leukemia (T-cell) Teratocarcinoma (seminiferous tubules) Microscopic hamartomatous polyps (colon)	++	+	+	–	–	+	+	+
9	32	*Lymphoma/leukemia (T-cell) Prostatic cancer (well differentiated) Microscopic hamartomatous polyps (colon)		++	+	–	–	–	–	–
(b) Treated with 5 Gy γ-radiation										
10	16	*Lymphoma/leukemia (T-cell) Microscopic hamartomatous polyps (jejunum)	++	+	+	+	+		+	+
11	16	*Lymphoma/leukemia (T-cell)	++	+	+	+	+	+	+	+
12	17	*Lymphoma/leukemia (T-cell) Microscopic hamartomatous polyps (colon)	++	+	+	–	+	+	+	+
13	19	*Lymphoma/leukemia (T-cell) Microscopic hamartomatous polyps (colon)	++	+	+	+	+		+	+
14	19	*Lymphoma/leukemia (T-cell) Microscopic hamartomatous polyps (colon)	++	+			+		+	+
15	21	*Lymphoma/leukemia (T-cell) Microscopic hamartomatous polyps (colon)	++	+	+		+		+	+

(a) In the untreated group, 66 heterozygous and 50 wild-type mice were observed for 20–36 weeks (mean 28 weeks). No tumors were observed in the wild-type mice. (b) In the group treated with γ-radiation, 32 heterozygous mice and 30 wild-type mice were observed for 19–21 weeks (mean 20 weeks). Mice at 5–6 weeks of age were treated with 5 Gy γ-radiation from a Cobalt 60 source at a dose rate of 1.095 Gy/min. No tumors were observed in wild-type mice. Symbols: +, infiltration of the lymphoma cells only; ++, gross organ enlargement and infiltration of the lymphoma cells; –, no evidence of lymphoma infiltrate or loss of heterozygosity (LOH). An asterisk indicates the main tumor; n.d. indicates not detected.

indicated by the abnormal expression of a number of regionalized markers, which is accompanied by an expansion of the neural folds and allantois. Thus, in *mPTEN*$^{3-5}$ mutant embryos, the excessive expansion of the allantois may impair its fusion to the chorion, affecting the process of placentation and therefore causing embryonic death. Mutations affecting chorio-allantoic fusion, such as *VCAM1*, allow embryonic survival until E10.5 [36,37], suggesting that impaired chorio-allantoic fusion is not the sole cause of death of *mPTEN*$^{3-5}$ mutants. Immunostaining showed that mPTEN distribution in embryonic tissue coincided with regions where differentiation occurs (data not shown). Thus, death of *mPTEN*$^{3-5}$ mutants by E9.5 is most likely to be caused by an imbalance between growth and patterning, which uncouples the timing of developmental events in mutant embryos. Interestingly, targeted inactivation of another tumor suppressor gene, *Nf1*, causes lethality before E14.5, which is associated with developmental abnormalities in different tissues [38,39], thus underscoring the importance of a tight regulation of growth and differentiation for normal development.

Figure 5

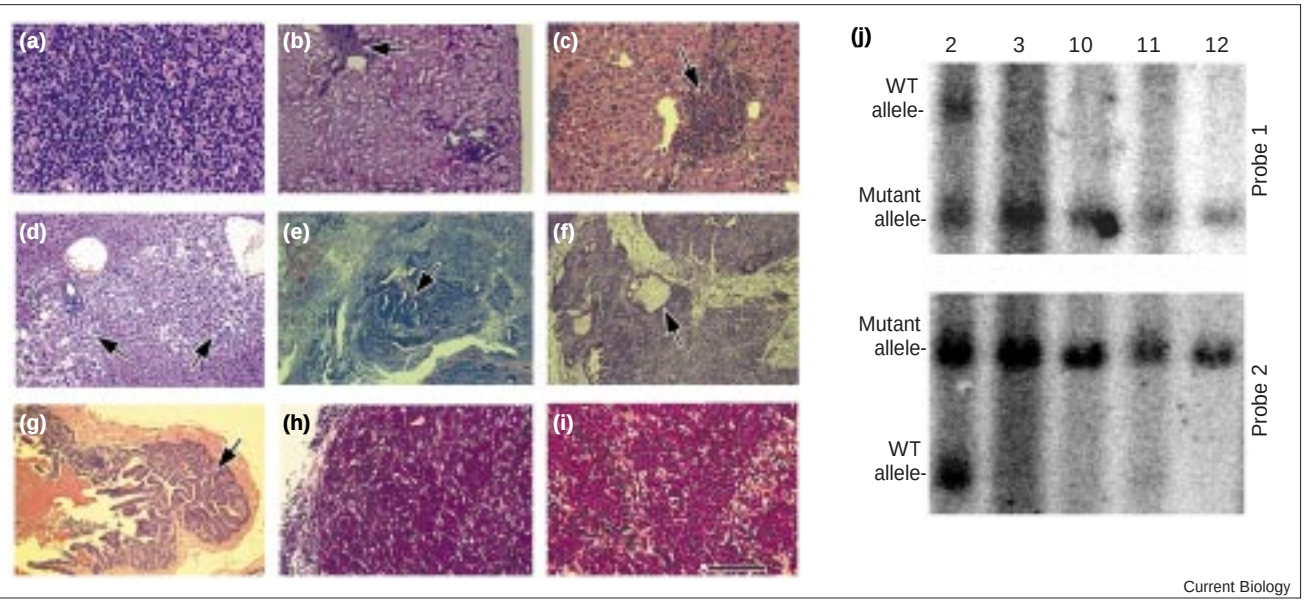

Tumors arising in *mPTEN*$^{3–5}$ heterozygous mice and loss of heterozygosity in T-cell lymphomas. **(a)** Lymph node. Normal tissue has been replaced by lymphoma infiltrate. **(b)** Kidney showing perivascular infiltration of leukemic cells (arrow). **(c,d)** Liver showing (c) infiltration of leukemic cells (arrow) and (d) atypical adenomatous hyperplasia (arrow). **(e,f)** Teratocarcinoma with primitive neural component (e, arrow). Atypical endodermal cells, blastocyst-like structures (f, arrow) and syncytiotrophoblast giant cells were also observed. **(g)** Prostatic gland showing well-differentiated carcinoma (arrow). **(h,i)** Thymus. Normal tissue has been replaced by lymphoma infiltrate. Bar in (i) represents 10 μm in (a–d,h,i); 40 μm in (e–g). **(j)** Loss of heterozygosity of *mPTEN* in tumors. Representative Southern blots of tumor DNA samples analyzed using the probe 1 (upper panel) and probe 2 (lower panel; see Figure 1a). DNA was digested with *Pvu*II (upper panel) or *Pst*I (lower panel). Complete loss of or a faint band of the wild-type allele was observed in some of the lymphoma/leukemia cases, as shown in Table 1.

Our findings are very different from those of Cristofano *et al.* [35] who were unable to find *mPTEN* mutant embryos after E7.5 and thus did not characterize the embryonic phenotype at all. We have deleted exons 3–5 of the *mPTEN* gene, and we have shown that the *mPTEN*$^{3–5}$ mutation is a lack-of-function mutation. Cristofano *et al.* deleted exons 4–5; therefore, it is unlikely that differences are caused by the nature of the mutations. In contrast, our analysis was mostly made in an outbred genetic background (CD1) whereas Cristofano *et al.* made their studies in an inbred background (129Sv and C57BL/J). Thus, phenotypic differences between the two *mPTEN* mutants may be attributed to the difference in genetic background.

Loss of heterozygosity in *mPTEN*$^{3–5}$ heterozygous mice leads to high tumor susceptibility

Our results show that heterozygous mice are highly susceptible to tumors, especially T-cell lymphoma/leukemia, that arise after loss of heterozygosity at the wild-type *mPTEN* locus. The frequency of the *PTEN* mutation in primary human lymphoma or leukemia is still unclear, but loss of heterozygosity has been reported in 48% of leukemia cell lines, some of which had mutations in *PTEN* as well [4]. We have also observed a relatively high incidence of teratocarcinomas in *mPTEN*$^{3–5}$ heterozygous mice and, although the 129 strain used in this study is prone to develop teratocarcinomas [40], we did not detect any teratocarcinomas in wild-type mice during the same period of observation. We also observed one case of well-differentiated prostatic cancer and three cases of atypical adenomatous hyperplasia in the liver. However, glioblastoma, endometrial cancer, thyroid cancer and breast cancer — in which sporadic or inherited (Cowden disease) *PTEN* mutations are found — were not observed in *mPTEN*$^{3–5}$ heterozygous mice. The frequency of tumor-bearing mice among *mPTEN*$^{3–5}$ heterozygotes seems to be much higher than in *p53* heterozygotes. In the case of *p53*, only 8% of heterozygous mice had tumors by 12 months of observation [41], whereas 14% of *mPTEN*$^{3–5}$ heterozygotes had tumors by seven months of observation, underscoring the importance of *mPTEN* in oncogenesis.

Cristofano *et al.* [35], have reported that *mPTEN* heterozygotes develop glandular hyperplasia in the colon, increased cellularity and mitotic figures in the prostatic gland, focal acanthosis in the skin, atrophic changes in the seminiferous tubules, and colon adenocarcinoma, teratoma, thyroid carcinoma and myeloid leukemia. This tumor spectrum is different from ours, as we mainly observe lymphomas, prostatic cancer, teratocarcinoma,

Figure 6

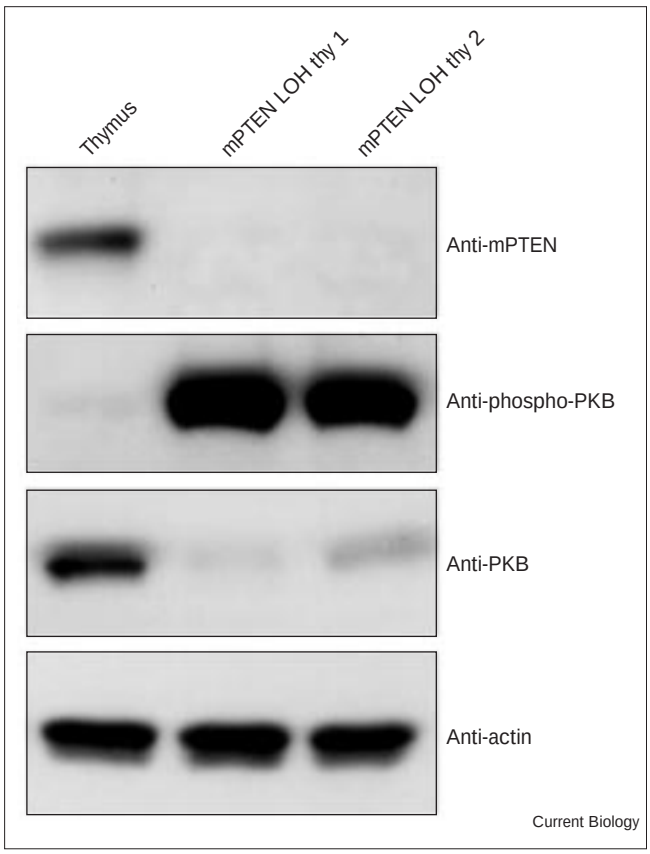

Increased phosphorylation of PKB/Akt in thymomas associated with *mPTEN* loss of heterozygosity (LOH). Western blot analyses of whole-cell extracts from normal mouse thymus and two thymomas (designated thy 1 and thy 2) derived from γ-irradiated *mPTEN* heterozygous mice. Antibodies used in western blots were to murine PTEN, PKB and its phosphorylated form, and actin.

hamartomatous polyps in the intestine and atrophic changes in the seminiferous tubules. We have not observed colon or thyroid cancers, nor myeloid leukemia, although we have found one instance of myeloid leukemia in heterozygous mice treated with the mutagen ethylnitrosourea (ENU). The differences in the types of tumors observed may be due to the following reasons. First, in our case tumors in *mPTEN* heterozygous mice arise as a consequence of the loss of heterozygosity of the wild-type *mPTEN* allele; in the work reported by Cristofano *et al.*, loss of heterozygosity at the *mPTEN* locus was not determined and tumors were attributed to *mPTEN* haplo-insufficiency [35]. Furthermore, tumors were observed in chimeric mice derived from *mPTEN* mutant ES cells and in *mPTEN* heterozygous mice, in which only colon carcinomas were found [35]. Second, the periods of observation are different, as in our case *mPTEN* heterozygotes were monitored for an average of 28 weeks; in Cristofano *et al.*, however, the chimeras were followed for 20 weeks, and the heterozygotes for 8 weeks [35]. Third, the genetic background may influence the type of tumors that originate, as in our case *mPTEN* heterozygous mice were mostly of an outbred CD1 background; in Cristofano *et al.* [35], the background was inbred 129Sv and C57BL/J.

The role of mPTEN in cellular survival and tumorigenesis

Our present data show that phosphorylation, and therefore activation, of Akt/PKB is significantly elevated in tumors generated by loss of heterozygosity at the *mPTEN* locus. We have found that Akt/PKB is activated even in the absence of stimulation in *mPTEN*$^{3-5}$-deficient embryonic fibroblasts, and apoptosis induced by ultraviolet (UV) radiation, osmotic stimuli or tumor necrosis factor-α (TNF-α) is inhibited in *mPTEN*$^{3-5}$-deficient embryonic fibroblasts [27]. Therefore, c-Akt appears to be a key target molecule in oncogenesis mediated by loss of heterozygosity at the wild-type *mPTEN* locus, as c-Akt hyperactivation may permit *mPTEN* mutant cells to acquire a survival advantage. Consistently, v-*akt*, the viral oncogene with a viral *gag* sequence fused to the entire open reading frame of murine Akt/PKB, causes T-cell lymphomas in mice [22]. Nevertheless, without testing thymic lymphomas from a different genetic background, it is still formally possible that the increased Akt levels observed in the thymic lymphomas of *mPTEN*$^{3-5}$ heterozygous mice may be an indirect effect of transformation. During embryogenesis, enhanced *Akt/PKB* activity cannot explain the phenotype observed in *mPTEN*$^{3-5}$ mutants, as we have not detected any reduction in apoptosis (data not shown), suggesting that, perhaps, alternate pathways involving PtdIns(3,4,5)P_3 may exist in the embryo.

The *mPTEN* gene is strongly expressed in thymus, and most of the loss of heterozygosity that we have observed was associated with thymic lymphomas. This would suggest that, in *mPTEN*$^{3-5}$ heterozygous mice, the double-strand breaks occurring during the T-cell receptor recombination process might affect the integrity of the wild-type *mPTEN* locus, an effect that would be accelerated by γ-irradiation. An alternative possibility is that, during the recombination process, the elimination of lymphocytes that accumulate abnormal intermediates may involve *mPTEN*, acting perhaps through the inhibition of the cell survival pathway mediated by *Akt/PKB*. Nevertheless, in preliminary experiments we were unable to detect a significant difference in irradiation-induced apoptosis between immortalized *mPTEN*$^{3-5}$-deficient and *mPTEN*$^{3-5}$ heterozygous control embryonic fibroblasts because, under our conditions (20 Gy irradiation dose), apoptosis was low in control cells. There may be significant differences in thymocyte apoptosis after γ-irradiation, however, which would be consistent with the accelerated rate with which thymomas arise in *mPTEN*$^{3-5}$ heterozygous mice after γ-irradiation. In humans, *PTEN* mutations were initially identified in glioblastomas [1]; therefore, the

question of whether *mPTEN* is involved in other cancers remains open. A longer observation period of *mPTEN* heterozygotes, or the generation of T-cell-specific or brain-specific *mPTEN*-deficient mice using the *cre–lox*P system will solve some of these questions.

Materials and methods

Generation of mPTEN-mutant ES cells and mice

The primers used for making the short arm of the targeting construct (see Figure 1a) were as follows: sense primer 5′-TACCGCGGGT-TAAAGATTCTTGGCCATTAC-3′; antisense primer 5′-ATGCGGC-CGCCTTACTACATCATCAATATTGTTC-3′. The construct was linearized by digestion with *Sac*II. Culture and transfection of ES cells were as described [42]. ES cell colonies resistant to G418 (250 mg/ml; Gibco) were screened for homologous recombination by PCR using primers specific for 5′ flanking sequences in the *mPTEN* and neomycin-resistance genes (sense primer a: 5′-GCCCTACA-GACTTTTTAATTTGTCTC-3′; antisense primer b: 5′-CAAGCAAAAC-CAAATTAAGGGCC-3′; Figure 1a), giving an amplified fragment of 925 bp. Recombinant clones were confirmed by Southern blotting using a 5′ flanking probe and a neomycin-specific probe to determine that homologous recombination occurred without random integrations. Chimeric mice were produced by microinjection using standard procedures. Germ-line transmission was obtained from three independent mutant ES cell lines that were injected into blastocysts. F2 offspring from heterozygous intercrosses were genotyped by genomic Southern blot (Figure 1b) or PCR analysis. The heterozygous males were crossed with CD1 or C57BL/6J mice.

PCR analysis of mPTEN$^{3–5}$ genotypes and phenotypes

Genomic DNA from ES cells and tails were isolated for PCR amplification following published protocols [43], and amplified by PCR (Figure 1b). Primer c (5′-ACAGACCTAGGCTACTGCTC-3′) and primer d (5′-CTAGAAGCAAGACTTCCGTTC-3′), specific for the deleted portion of the *mPTEN* gene, were used to detect the wild-type allele, while primer e (5′-TGCTATGGGATTTCCTGCAG-3′) and primer b (see above) were used to detect the mutant allele (Figure 1a). The PCR cycling conditions were 50 cycles of 94°C 1 min, 64°C 1 min and 72°C 1 min. Primer pair c/d amplified a 669 bp fragment in both heterozygous and wild-type DNA samples, whereas the primer pair e/b amplified a 144 bp fragment in both heterozygous and homozygous mutant DNA.

Histological analysis

Embryos were dissected and processed according to standard protocols [43].

Whole-mount in situ *hybridization*

E8.5 embryos were isolated in ice-cold PBS, fixed overnight in 4% paraformaldehyde and processed for whole-mount *in situ* hybridization following published procedures [44]. The probes used were *Mox1* [31], *Krox20* [30], *Wnt1* [32] and *Wnt3a* [33].

Radioactive in situ *hybridization*

Embryos were processed as for histological analysis. The probes used were Brachyury and *Mash-2* [28]. Probes were labelled with [^{32}P]UTP and processed according to described protocols [45].

Analysis of tumors from mPTEN$^{3–5}$ heterozygous mice

Autopsy was performed on all moribund mice or mice with visible tumors. Specimens were fixed in 10% buffered formalin and embedded in paraffin, or snap frozen in liquid nitrogen and stored at –70°C. For histological analysis sections 5 μm thick were cut and stained with hematoxylin and eosin. Immunosurface staining from single-cell tumor suspensions were performed according to standard methods, using antibodies against T-cell receptor, CD4, CD8, B220, CD19 and Gr-1 (Pharmingen).

γ-Irradiation of mPTEN$^{3–5}$ heterozygous mice

Thirty-two heterozygous, and 30 wild-type mice at 5–6 weeks of age were exposed to a single dose of 5 Gy whole-body irradiation from a Cobalt 60 source (Gammacell40 Exactor, Nordion International Inc.) at a dose rate of 1.095 Gy/min.

Western blot analysis

Proteins were resolved by SDS–PAGE on 12.5% gels, electroblotted to PVDF membrane (Boehringer Manheim), blocked in 4% skim milk, 1 × PBS, 0.05% Tween-20 and probed with primary antibodies. Anti-PTEN [27], anti-phosphoS473 Akt/PKB and anti-Akt/ PKB antibodies are from New England Biolabs and anti-actin antibody from Sigma. Following incubation with horseradish peroxidase-conjugated goat anti-rabbit antibody (Amersham), bound immunoglobulins were detected using enhanced chemiluminescence (Amersham).

Acknowledgements

We thank Ritsuko Yoshida, Annette van der Heiden, Christine Mirtsos, Tom Graves, Andrew Hessel and David Siderovski for technical assistance and helpful information; Mary Saunders and Alex Grossman for critical reading of the manuscript and Miki Sato for her support.

References

1. Li J, Yen C, Liaw D, Podsypanina K, Bose S, Wang SI, *et al.*: PTEN, a putative protein tyrosine phosphatase gene mutated in human brain, breast, and prostate cancer. *Science* 1997, 275:1943-1947.
2. Steck PA, Pershouse MA, Jasser SA, Yung WK, Lin H, Ligon AH, *et al.*: Identification of a candidate tumour suppressor gene, MMAC1, at chromosome 10q23 3 that is mutated in multiple advanced cancers. *Nat Genet* 1997, 15:356-362.
3. Li DM, Sun H: TEP1, encoded by a candidate tumor suppressor locus, is a novel protein tyrosine phosphatase regulated by transforming growth factor beta. *Cancer Res* 1997, 57:2124-2129.
4. Teng DHF, Hu R, Lin H, Davis T, Iliev D, Frye C, *et al.*: MMAC1/PTEN mutations in primary tumor specimens and tumor cell lines. *Cancer Res* 1997, 57:5221-5225.
5. Bostrom J, Cobbers JM, Wolter M, Tabatabai G, Weber RG, Lichter P, *et al.*: Mutation of the PTEN (MMAC1) tumor suppressor gene in a subset of glioblastomas but not in meningiomas with loss of chromosome arm 10q. *Cancer Res* 1998, 58:29-33.
6. Rasheed BK, Stenzel TT, McLendon RE, Parsons R, Friedman AH, Friedman HS, *et al.*: PTEN gene mutations are seen in high-grade but not in low-grade gliomas. *Cancer Res* 1997, 57:4187-4190.
7. Feilotter HE, Nagai MA, Boag AH, Eng C, Mulligan LM: Analysis of PTEN and the 10q23 region in primary prostate carcinomas. *Oncogene* 1998, 16:1743-1748.
8. Wang SI, Parsons R, Ittmann M: Homozygous deletion of the PTEN tumor suppressor gene in a subset of prostate adenocarcinomas. *Clin Cancer Res* 1998, 4:811-815.
9. Kohno T, Takahashi M, Manda R, Yokota J: Inactivation of the PTEN/MMACI/ITEPI gene in human lung cancers. *Genes Chromosomes Cancer* 1998, 22:152-156.
10. Tashiro H, Blazes MS, Wu R, Cho KR, Bose S, Wang SI, *et al.*: Mutations in PTEN are frequent in endometrial carcinoma but rare in other common gynecological malignancies. *Cancer Res* 1997, 57:3935-3940.
11. Risinger JI, Hayes AK, Berchuck A, Barrett JC: PTEN/MMAC1 mutations in endometrial cancers. *Cancer Res* 1997, 57:4736-4738.
12. Rhei E, Kang L, Bogomolniy F, Federici MG, Borgen PI, Boyd J: Mutation analysis of the putative tumor suppressor gene PTEN/MMAC1 in primary breast carcinomas. *Cancer Res* 1997, 57:3657-3659.
13. Singh B, Ittmann MM, Krolewski JJ: Sporadic breast cancers exhibit loss of heterozygosity on chromosome segment 10q23 close to the Cowden disease locus. *Genes Chromosomes Cancer* 1998, 21:166-171.
14. Peters N, Wellenreuther R, Rollbrocker B, Hayashi Y, Meyer-Puttlitz B, Duerr EM, *et al.*: Analysis of the PTEN gene in human meningiomas. *Neuropathol Appl Neurobiol* 1998, 24:3-8.
15. Suzuki H, Freije D, Nusskern DR, Okami K, Cairns P, Sidransky D, *et al.*: Interfocal heterogeneity of PTEN/MMAC1 gene alterations in multiple metastatic prostate cancer tissues. *Cancer Res* 1998, 58:204-209.

16. Liaw D, Marsh DJ, Li J, Dahia PL, Wang SI, Zheng Z, *et al.*: Germline mutations of the PTEN gene in Cowden disease, an inherited breast and thyroid cancer syndrome. *Nat Genet* 1997, 16:64-67.
17. Nelen MR, van Staveren WC, Peeters EA, Hassel MB, Gorlin RJ, Hamm H, *et al.*: Germline mutations in the PTEN/MMAC1 gene in patients with Cowden disease. *Hum Mol Genet 1997,* 6:1383-1387.
18. Eng C: Genetics of Cowden syndrome: through the looking glass of oncology. *Int J Oncol* 1998, 12:701-710.
19. Myers MP, Tonks NK: PTEN: sometimes taking it off can be better than putting it on. *Am J Hum Genet* 1997, 61:1234-1238.
20. Maehama T, Dixon JE: The tumor suppressor, PTEN/MMAC1, dephosphorylates the lipid second messenger, phosphatidylinositol 3,4,5-trisphosphate. *J Biol Chem* 1998, 273:13375-13378.
21. Dudek H, Datta SR, Franke TF, Birnbaum MJ, Yao R, Cooper GM, *et al.*: Regulation of neuronal survival by the serine-threonine protein kinase Akt. *Science* 1997, 275:661-5.
22. Staal SP, Hartley JW: Thymic lymphoma induction by the AKT8 murine retrovirus. *J Exp Med* 1988 167:1259-64.
23. Furnari FB, Lin H, Huang HJS, Cavenee WK: Growth suppression of glioma cells by PTEN requires a functional phosphatase catalytic domain. *Proc Natl Acad Sci USA* 1997, 94:12479-12484.
24. Tamura M, Gu J, Matsumoto K, Aota S, Parsons R, Yamada KM: Inhibition of cell migration, spreading, and focal adhesions by tumor suppressor PTEN. *Science* 1998, 280:1614-1617.
25. Marsh DJ, Coulon V, Lunetta KL, Rocca-Serra P, Dahia PL, Zheng Z, *et al.*: Mutation spectrum and genotype-phenotype analyses in Cowden disease and Bannayan-Zonana syndrome, two hamartoma syndromes with germline PTEN mutation. *Hum Mol Genet* 1998, 7:507-515.
26. Kispert A, Herrmann BG: The Brachyury gene encodes a novel DNA binding protein. *EMBO J* 1993, 12:3211-20.
27. Stambolic V, Suzuki A, de la Pompa JL, Brothers GM, Mirtsos C, Sasaki T, *et al.*: Negative regulation of PKB/Akt-dependent cell survival by the tumor suppressor PTEN. *Cell* 1998, 95:29-39.
28. Guillemot F, Nagy A, Auerbach A, Rossant J, Joyner AL: Essential role of Mash-2 in extraembryonic development. *Nature* 1994, 371:333-6.
29. Rossant J: Development of the extraembryonic lineages. *Semin Dev Biol* 1995 6:237-247.
30. Wilkinson DG, Bhatt S, Chavrier P, Bravo R, Charnay P: Segment-specific expression of a zinc-finger gene in the developing nervous system of the mouse. *Nature* 1989, 337:461-464.
31. Candia AF, Hu J, Crosby J, Lalley PA, Noden D, Nadeau JH, Wright CV: Mox-1 and Mox-2 define a novel homeobox gene subfamily and are differentially expressed during early mesodermal patterning in mouse embryos. *Development* 1992, 116:1123-36.
32. Wilkinson DG, Bailes JA, McMahon AP: Expression of the proto-oncogene int-1 is restricted to specific neural cells in the developing mouse embryo. *Cell* 1987, 50:79-88.
33. Takada S, Stark KL, Shea MJ, Vassileva G, McMahon JA, McMahon AP: Wnt-3a regulates somite and tailbud formation in the mouse embryo. *Genes Dev* 1994, 8:174-89.
34. Widmann C, Gibson S, Johnson GL: Caspase-dependent cleavage of signaling proteins during apoptosis A turn-off mechanism for anti-apoptotic signals. *J Biol Chem* 1998, 273:7141-7.
35. Cristofano AD, Pesce B, Cordon-Cardo C, Pandolfi PP: PTEN is essential for embryonic development and tumour suppression. *Nat Genet* 1998, 19:348-355.
36. Gurtner GC, Davis V, Li H, McCoy MJ, Sharpe A, Cybulsky MI: Targeted disruption of the murine VCAM1 gene: essential role of VCAM-1 in chorio-allantoic fusion and placentation. *Genes Dev* 1995, 9:1-14.
37. Kwee L, Baldwin HS, Shen HM, Stewart CL, Buck C, Buck CA, Labow MA: Defective development of the embryonic and extraembryonic circulatory systems in vascular cell adhesion molecule (VCAM-1) deficient mice. *Development* 1995, 121:489-503.
38. Brannan CI, Perkins AS, Vogel KS, Ratner N, Nordlund ML, Reid SW, *et al.*: Targeted disruption of the neurofibromatosis type-1 gene leads to developmental abnormalities in heart and various neural crest-derived tissues. *Genes Dev* 1994, 8:1019-1029.
39. Jacks T, Shih TS, Schmitt EM, Bronson RT, Bernards A, Weinberg RA: Tumour predisposition in mice heterozygous for a targeted mutation in Nf1. *Nat Genet* 1994, 7:353-361.
40. Wang D, Enders GC: Expression of a specific mouse germ cell nuclear antigen (GCNA1) by early embryonic testicular teratoma cells in 129/Sv-SI/+ mice. *Cancer Lett* 1996, 100:31-36.
41. Harvey M, McArthur MJ, Montgomery CA Jr, Butel JS, Bradley A, Donehower LA: Spontaneous and carcinogen-induced tumorigenesis in p53-deficient mice. *Nat Genet* 1993, 5:225-229.
42. Suzuki A, Andrew DP, Gonzalo JA, Fukumoto M, Spellberg J, Hashiyama M: CD34-deficient mice have reduced eosinophil accumulation after allergen exposure and show a novel crossreactive 90-kD protein. *Blood* 1996, 87:3550-3562.
43. Suzuki A, de la Pompa JL, Hakem R, Elia A, Yoshida R, Mo R, *et al.*: Brca2 is required for embryonic cellular proliferation in the mouse. *Genes Dev* 1997, 11:1242-1252.
44. Koop KE, MacDonald LM, Lobe CG: Transcripts of Grg4, a murine groucho-related gene, are detected in adjacent tissues to other murine neurogenic gene homologues during embryonic development. *Mech Dev* 1996, 59:73-87.
45. Hui CC, Joyner AL: A mouse model of greig cephalopolysyndactyly syndrome: the extra-toesJ mutation contains an intragenic deletion of the Gli3 gene. *Nat Genet* 1993, 3:241-246.

Because *Current Biology* operates a 'Continuous Publication System' for Research Papers, this paper has been published on the internet before being printed. The paper can be accessed from http://biomednet.com/cbiology/cub – for further information, see the explanation on the contents page.